Synthesis and characterization of oxorhenium(V)–catecholate complexes. Crystal and molecular structures of $(CH_3)_4N[ReO(O_2C_6H_4)_2]$ and $(CH_3)_4N[ReO(PPh_3)(O_2C_6H_4)_2]\cdot CH_3OH$

Peter B. Kettler, Yuan-Da Chang and Jon Zubieta*
Department of Chemistry, Syracuse University, Syracuse, NY 13244 (USA)

Michael J. Abrams
Johnson Matthey, Metallopharmaceuticals Research, 1401 King Road, West Chester, PA 19380 (USA)

(Received October 22, 1993; revised December 21, 1993)

Abstract

The reactions of $ReOCl_3(PPh_3)_2$ with catechol and substituted catechols in methanol in the presence of triethylamine and tetramethylammonium chloride under N_2 yield the green complexes $[(CH_3)_4N]^+[ReO(cat)_2(PPh_3)]^-$ (cat = $O_2C_6H_4$ (**2**), 4-CH_3-$O_2C_6H_3$ (**3**), $O_2C_6Cl_4$ (**4**)). The reactions of **2** and **3** with pyridine in methylene chloride yield $[(CH_3)_4N]^+[ReO(cat)_2(py)]^-$ (**5**) and $[(CH_3)_4N]^+[ReO(4\text{-Me-cat})_2(py)]^-$ (**6**). Variable temperature ^1H and ^{31}P NMR spectroscopy studies on these complexes indicate that the ancillary ligands (PPh_3: **2**, **3**; py: **5**, **6**) undergo a dissociation–association process in solution along with concomitant *cis–trans* isomerization of the catecholate ligands. The reaction of $[(CH_3CH_2)_4N]^+[ReO_2(cat)_2]^-$ (**8**) with triphenylphosphine in refluxing ethanol yields the reduced rhenium(V) square pyramidal complex $[(CH_3CH_2)_4N]^+[ReO(cat)_2]^-$ (**7**) as an air and moisture-sensitive tan solid where triphenylphosphine acts as a reducing agent. These complexes were characterized by elemental analysis, variable temperature ^1H and ^{31}P NMR spectroscopy and IR and UV–Vis spectroscopies. Complexes **2** and **7** were also characterized by X-ray crystallography. Crystal data: $C_{20}H_{28}NO_5Re$ (**2**): tetragonal space group *I4/m*, $a = 19.890(3)$, $c = 10.438(2)$ Å, $V = 4129(2)$ Å^3, $Z = 8$, $D_{calc} = 1.766$ g cm^{-3}; structure solution and refinement based on 976 reflections (Mo Kα, $\lambda = 0.71073$ Å) converged at $R = 0.043$. $C_{36}H_{43}NO_7PPe$ (**7**): monoclinic space group *C2/c*, $a = 25.485(5)$ Å, $b = 9.127(2)$, $c = 30.590(6)$ Å, $\beta = 101.84(3)°$, $V = 6964(3)$ Å^3, $Z = 8$, $D_{calc} = 1.563$ g cm^{-3}; 3298 reflections, $R = 0.047$.

Key words: Crystal structures; Rhenium complexes; Oxo complexes; Catecholate complexes

Introduction

Catechols and catecholate ligands are of interest due to their significance in certain biological systems and their inherent redox activity. Particular biological systems where catechols participate include their incorporation in iron sequestering agents (siderophores) such as enterobactin [1] and also as biogenic amines such as the catecholamines adrenaline, dopamine and isoprotenerol which act as neurotransmitters in the brain and nervous systems of mammals [2, 3].

Specifically of interest to us are rhenium and technetium catecholate complexes because of the utilization of ^{186}Re and ^{99m}Tc radionuclides in radiopharmaceuticals. Known technetium catecholate complexes include the Tc(V) oxo–catecholate anions $[Bu_4N]^+[TcO(cat)_2]^-$ [4] and $[Bu_4N]^+[TcO(Cl_4cat)_2]^-$ [5], the neutral Tc(VI) complexes $Tc(DBcat)_3$ and $Tc(DBcat)_2(DBAP)$ [6] and the unusual Tc(V)/Tc(VI) mixed valence complex $[Bu_4N]^+[Tc_2(N_2Ph_2)_2(Cl_4cat)_4]^-$ [4]. Known rhenium–catecholate complexes include the congeners of the Tc(VI) complexes $Re(DBcat)_3$ and $Re(Cl_4cat)_3$ [7], a variety of organometallic rhenium–catecholate complexes reported by Herrmann and co-workers ($[Cp^*Re(Cl_4cat)_2]$, $ReMeO_2(cat)(py)$, $ReMeO_2(phencat)(py)$, $[C_5H_5NH]^+[ReMeO_2(cat)(X)]^-$ (X = Cl, Br, I)) [8–10] and more recently, the complexes $ReOCl(cat)(PPh_3)_2$, $[Bu_4N]^+[ReO(X_4cat)_2(py)]^-$ (X = Cl, Br), $[Bu_4N]^+[ReO(X_4cat)_2(MeOH)]^-$ reported by Griffith and coworkers [11], the complexes $[(CH_3)_4N]^+[ReO(cat)_2]^-$

*Author to whom correspondence should be addressed.

SSDI 0020-1693(94)03809-3

(**1**) and $[(CH_3CH_2)_4N]^+[ReO_2(cat)_2]^-$ (**8**) reported by Dilworth *et al.* [12] and the Re(V) species $(HBpz_3)$-ReO(9,10-phenanthrene-diolate) [13].

Recently, we have explored the coordination chemistry of technetium organohydrazine complexes to model the uptake of ^{99m}Tc by a bifunctional hydrazine reagent [4, 14–17]. Tc(V) oxo precursors were found to add readily under mild conditions to hydrazinopyridine-modified proteins to yield stable ^{99m}Tc-labeled proteins in >90% radiometric yield [18]. ^{99m}Tc-hydrazinopyridine polyclonal IgG conjugates have been demonstrated to be useful agents for the imaging of focal sites of infection [19]. Since we have studied the reactivity of Tc(V) oxo–catecholates as models for $[TcO(gluco-heptonate)_2]^-$, a common synthetic precursor in the preparation of ^{99m}Tc protein conjugates, we deemed it necessary to examine the analogous Re(V) oxo–catecholates due to the utility of the ^{186}Re radionuclide in therapeutic radiopharmaceuticals.

Upon perusal of the literature, the $[(CH_3)_4N]^+[ReO(cat)_2]^-$ (**1**) complex seemed to be an ideal precursor to study the reactivity of Re(V) oxo–catecholates with organohydrazines [12]. However, upon the attempted preparation of this oxo-catecholate precursor, the olive-green solid described was not the $[(CH_3)_4N]^+[ReO(cat)_2]^-$ (**1**) complex reported [12], but actually the six-coordinate complex $[(CH_3)_4N]^+[ReO(cat)_2(PPh_3)]^-$ (**2**). Other derivatives of this complex with different catecholate ligands such as 4-methyl-catechol and tetrachlorocatechol (**3**, **4**) and with pyridine (C_5H_5N) as a different ancillary ligand (**5**, **6**) were prepared and are reported herein. These complexes are completely characterized by elemental analysis, IR and UV–Vis spectroscopy, multinuclear (^{1}H and ^{31}P) NMR spectroscopy at variable temperatures and an X-ray crystal structure of **2**. The $ReO(cat)_2^-$ anion (**7**) was isolated as a tan solid upon the reduction of $[(CH_3CH_2)_4N]^+[ReO_2(cat)_2]^-$ (**8**) with PPh_3. This complex was also characterized spectroscopically and structurally as described above. However, these complexes react with organohydrazines to only form intractable solids. Further reactivity of organohydrazines with other rhenium oxo–catecholates will be reported at a later date [20].

Experimental

General considerations

NMR spectra were recorded on the General Electric QE 300 (^{1}H, 300.10 MHz; ^{13}C, 75.47 MHz) and Bruker AMX 300 (^{31}P, 121.35 MHz) Fourier transform spectrometers in CD_3OD (3.30 ppm), CD_2Cl_2 (5.32 ppm) or CD_3CN (1.93 ppm). Variable temperature ^{1}H NMR spectra were measured on the General Electric QE 300 spectrometer utilizing a Doric Trendicator 410A temperature controller while ^{31}P variable temperature NMR spectra were measured on the Bruker AMX 300 spectrometer utilizing a Eurotherm temperature controller. IR spectra were recorded as KBr pellets with a Perkin-Elmer 1600 Series FTIR. UV–Vis spectra were recorded on a Cary 1E spectrophotometer. Elemental analyses for carbon, hydrogen and nitrogen were carried out by Oneida Research Services, Whitesboro, NY.

All synthetic manipulations were carried out utilizing standard Schlenk techniques while most spectroscopic preparations were performed in a Vacuum Atmospheres TS-5000 glovebox equipped with a MO-20 drytrain. Solvents were distilled from their appropriate drying agents [21]. Pyridine (Fisher) and triethylamine (Aldrich) were distilled from CaH_2 and stored under an inert atmosphere. Methanol (Sure-Seal; Aldrich), ethanol (Sure-Seal; Aldrich), catechol (Aldrich), 4-methyl-catechol (Aldrich), tetrachlorocatechol (Aldrich), PPh_3 (Aldrich), $(CH_3)_4NCl$ (Aldrich), $(CH_3CH_2)_4NCl$ (Aldrich) and other reagents were used as received without further purification. $ReOCl_3(PPh_3)_2$ [22] was synthesized by a published procedure and $[(CH_3CH_2)_4N]^+[ReO_2(cat)_2]^-$ (**8**) was synthesized by a modification of a published procedure [12, 20].

X-ray crystallographic studies

The crystal parameters for the X-ray structures of **2** and **7** are summarized in Table 1. See also 'Supplementary material'. Data for both **2** and **7** were collected at −60 °C and corrected in the usual fashion for Lorentz, polarization, and absorption effects. Both structures were solved by the heavy-atom method. All non-hydrogen atoms were refined anisotropically, while hydrogen atoms were introduced as fixed contributors in idealized positions. Both structures exhibited partially disordered cations, whose geometries were optimized and refined subject to C–N distance constraints. Atomic positional parameters are listed in Tables 2 and 3, and bond lengths and angles are presented in Tables 4 and 5 for **7** and **2**, respectively. While the cation disorder must inevitably affect all metrical parameters associated with the structures, specifically the estimated standard derivatives in bond lengths and angles, it should be stressed that the anions are well-behaved. Consequently, comparisons of structural parameters to those observed for related structures are valid within the conventional limits imposed by the uncertainties defined by the e.s.d.s.

$[(CH_3)_4N]^+[ReO(cat)_2(PPh_3)]^-$ (2)

A suspension of $ReOCl_3(PPh_3)_2$ (6.000 g, 7.20 mmol), catechol (1.566 g, 14.22 mmol) and triethylamine (5.679 g, 57.02 mmol) was heated to reflux in 130 ml of anhydrous methanol. Upon heating, the yellow–green suspension became a dark green homogeneous reaction

TABLE 1. Summary of crystal data for the structures of $(C_2H_5)_4N[ReO(O_2C_6H_4)_2]$ (7) and $(CH_3)_4N[ReO(O_2C_6H_4)_2(PPh_3)]\cdot 2CH_3OH$ (2)

Formula	$C_{20}H_{28}NO_5Re$	$C_{36}H_{43}O_7NPRe$
Formula weight	548.7	818.9
a (Å)	19 890(3)	25.485(5)
b (Å)		9.127(2)
c (Å)	10.438(2)	30.590(6)
β (°)		101.84(3)
V (Å^3)	4129(2)	6964(3)
Z	8	8
D_{calc} (g cm^{-1})	1.766	1.563
Space group	$I4/m$	$C2/c$
Absorption coefficient (Mo Kα) (cm^{-1})	59.10	35.84
No. of reflections, $I_o \geqslant 3\sigma(I_o)$	976	3298
R[a]	0.0431	0.0465
R_w[b]	0 0502	0.0530

[a]$\Sigma||F_o|-|F_c||/\Sigma|F_o|$. [b]$[\Sigma w(|F_o|-|F_c|)^2/\Sigma w|F_o|^2]^{1/2}$.

TABLE 2. Atomic coordinates ($\times 10^4$) and equivalent isotropic displacement coefficients (Å$^2\times 10^3$) for 7

	x	y	z	U_{eq}[a]
Re(1)	3539(1)	1479(1)	0	39(1)
N(1)	1373(9)	3613(10)	0	45(7)
O(1)	4243(8)	1025(8)	0	55(6)
O(2)	2885(5)	1118(5)	1227(10)	44(4)
O(3)	3615(6)	2221(5)	1231(9)	48(4)
C(1)	2401(7)	736(7)	663(14)	40(5)
C(2)	1921(8)	379(8)	1377(16)	53(6)
C(3)	1445(8)	19(8)	711(15)	54(6)
C(4)	3794(8)	2818(7)	702(13)	42(5)
C(5)	3947(7)	3391(7)	1378(16)	48(5)
C(6)	4114(8)	3967(8)	744(16)	55(7)
C(7)	1056(17)	4074(18)	1182(35)	55(9)
C(8)	444(10)	3760(10)	1680(19)	71(5)
C(9)	1371(35)	2956(34)	938(65)	153(25)
C(10)	2456(21)	−1940(22)	0	117(13)
C(11)	1842(25)	3934(26)	906(51)	96(15)
C(12)	2343(19)	4396(19)	−226(54)	86(16)

[a]Equivalent isotropic U defined as one third of the trace of the orthogonalized U_{ij} tensor.

mixture. After 3 h of refluxing, $(CH_3)_4NCl$ (4.617 g, 42.14 mmol) dissolved in 30 ml methanol was added to the reaction mixture and cooled to 25 °C. Upon stirring for 12 h, an olive-green solid precipitated from solution. The product was collected, washed with methanol and dried *in vacuo* (4.518 g, 5.98 mmol, 83%). *Anal.* Calc. for $C_{34}H_{35}NO_5PRe$ (mol. wt. 754.85): C, 54.10; H, 4.67; N, 1.86. Found: C, 54.07; H, 4.52; N, 1.74%. IR (KBr): 3050(m), 1576(w), 1471(vs), 1435(m), 1334(w), 1274(m), 1255(s), 1237(vs), 1190(w), 1096(m), 1018(w), 941(s), 794(s), 752(s), 695(s), 643(m), 622(m), 528(s). ^{1}H NMR (CD_2Cl_2, 293 K): δ 7.33 (br, 15H); 7.0 (br, 4H); 6.6 (br, 4H); 3.13 (s, 12H); ^{1}H NMR (CD_2Cl_2, 223 K): δ 7.42 (m, 15H); 7.11 (br m, 1H); 6.65 (m, 4H); 6.39 (t, J=7.7 Hz, 1H); 6.03 (t, J=7.7 Hz, 1H); 5.58 (d, J=7.5 Hz, 1H); 3.13 (s, 12H). ^{31}P NMR (CD_2Cl_2, 300 K): δ −5.2 (br); ^{31}P NMR (CD_2Cl_2, 223 K): δ −16.8 (s). UV–Vis (λ_{max} (nm) (ϵ (M^{-1} cm^{-1})) in CH_3OH): 220 (2300); 268 (2700); 450 (sh); 647 (100).

$[(CH_3)_4N]^+[ReO(4\text{-Me-cat})_2(PPh_3)]^-$ (3)

A solution of $ReOCl_3(PPh_3)_2$ (4.000 g, 4.80 mmol), 4-methyl-catechol (1.176 g, 9.48 mmol) and triethylamine (3.846 g, 38.01 mmol) was reacted with $(CH_3)_4NCl$ (3.048 g, 28.09 mmol) as described for **2**. An olive-green product was collected (3.270 g, 4.18 mmol, 87%). *Anal.* Calc. for $C_{36}H_{39}NO_5PRe$ (mol. wt. 782.94): C, 54.53; H, 5.31; N, 1.72. Found: C, 53.97; H, 5.05; N, 1.85%. IR (KBr): 3355(br, w), 3025(w), 2918(vw), 1570(w), 1485(vs), 1435(m), 1379(w), 1251(s), 1214(m), 1116(vw), 1098(m), 1018(w), 998(vw), 937(s), 848(w), 812(s), 747(m), 697(s), 666(m), 649(m), 634(w), 530(s). ^{1}H NMR (CD_2Cl_2, 293 K): δ 7.3 (br, 15H); 6.8 (br, 2H); 6.4 (br, 4H), 3.11 (s, 12H); 2.2 (br, 6H); ^{1}H NMR (CD_2Cl_2, 223 K): δ 7.41 (m); 7.00 (d, J=7.8 Hz); 6.94 (s); 6.92 (s); 6.88 (s); 6.54 (br m); 6.32 (d, J=6.1 Hz); 6.18 (d, J=8.0 Hz); 5.86 (d, J=7.6 Hz); 5.52 (dd); 5.22 (s); 3.11 (s); 2.10 (s); 1.93 (s). ^{31}P NMR (CD_2Cl_2, 300 K): δ −5.1; ^{31}P NMR (CD_2Cl_2, 223 K): δ −16.7 (1P); −16.8 (2P); −17.0 (1P). UV–Vis (λ_{max} (nm) (ϵ (M^{-1} cm^{-1})) in CH_3OH): 230 (2000); 350 (sh); 530 (150).

$[(CH_3CH_2)_3NH]^+[ReO(Cl_4cat)_2(PPh_3)_2]^-$ (4)

A suspension of $ReOCl_3(PPh_3)_2$ (5.000 g, 6.00 mmol), tetrachlorocatechol (2.900 g, 11.70 mmol) and triethylamine (4.796 g, 46.91 mmol) was heated to reflux as described for **2**. After 2 h, an olive-green solid precipitated from the reaction mixture. The product was collected by filtration, washed with methanol and dried *in vacuo* (4.520 g, 4.62 mmol, 77%). *Anal.* Calc. for $C_{36}H_{31}Cl_8NO_5PRe$ (mol. wt. 978.46): C, 40.85; H, 2.95; N, 1.32. Found: C, 40.84; H, 2.80; N, 1.28%. IR (KBr): 3027(m), 2898(w), 2725(w), 1541(w), 1484(sh), 1474(sh), 1443(s), 1411(vs), 1378(s), 1285(w), 1248(w), 1098(m),

TABLE 3. Atomic coordinates ($\times 10^4$) and equivalent isotropic displacement coefficients ($Å^2 \times 10^3$) for **2**

	x	y	z	U_{eq}[a]
Re(1)	1278(1)	6835(1)	1685(1)	29(1)
P(1)	788(1)	6099(3)	935(1)	28(1)
O(1)	909(3)	8391(9)	1619(3)	42(3)
O(2)	1717(3)	5047(8)	1580(2)	28(3)
O(3)	1956(3)	7744(8)	1527(3)	37(3)
O(4)	847(3)	5486(9)	1975(3)	36(3)
O(5)	1690(3)	7028(9)	2323(2)	38(3)
N(1)	1716(4)	1545(10)	2342(3)	36(3)
C(1)	2146(5)	5302(13)	1400(4)	31(3)
C(2)	2278(5)	6788(14)	1383(4)	37(3)
C(3)	2752(5)	7161(15)	1238(4)	46(3)
C(4)	3061(6)	6043(16)	1105(5)	56(4)
C(5)	2910(6)	4627(18)	1108(5)	61(4)
C(6)	2451(5)	4237(14)	1256(4)	41(3)
C(7)	975(5)	5536(14)	2426(4)	38(3)
C(8)	1419(5)	6352(12)	2615(4)	31(3)
C(9)	1585(5)	6472(14)	3074(4)	42(3)
C(10)	1302(5)	5710(15)	3342(5)	50(4)
C(11)	874(6)	4870(16)	3161(5)	56(4)
C(12)	709(5)	4769(15)	2698(4)	49(3)
C(13)	155(4)	7122(12)	773(3)	26(3)
C(14)	−162(4)	7318(12)	1086(4)	32(3)
C(15)	−634(5)	8120(15)	976(4)	43(3)
C(16)	−778(5)	8744(15)	559(4)	47(3)
C(17)	−467(5)	8579(14)	256(4)	43(3)
C(18)	4(5)	7767(13)	351(4)	36(3)
C(19)	585(4)	4182(12)	931(3)	27(3)
C(20)	75(5)	3793(14)	952(4)	40(3)
C(21)	−47(6)	2284(16)	984(4)	54(4)
C(22)	334(5)	1234(16)	990(4)	48(3)
C(23)	834(5)	1624(15)	958(4)	45(3)
C(24)	977(5)	3119(14)	925(4)	40(3)
C(25)	1113(5)	6266(14)	460(4)	35(3)
C(26)	1011(5)	5280(15)	105(4)	45(3)
C(27)	1272(6)	5405(17)	−246(5)	61(4)
C(28)	1629(6)	6508(17)	−246(5)	63(4)
C(29)	1726(6)	7523(17)	89(5)	59(4)
C(30)	1473(5)	7408(14)	449(4)	43(3)
C(31)	1956(5)	2952(14)	2553(4)	44(3)
C(32)	1993(6)	1107(17)	1984(5)	59(4)
C(33)	1134(5)	1787(16)	2140(4)	48(3)
C(34)	1757(6)	382(17)	2682(5)	65(4)
C(35)	192(5)	8955(15)	2797(4)	51(4)
C(36)	2301(8)	2017(23)	119(6)	97(6)
O(6)	310(4)	178(12)	2977(3)	72(3)
O(7)	2299(7)	1192(20)	492(6)	142(6)

[a]Equivalent isotropic U defined as one third of the trace of the orthogonalized U_{ij} tensor.

992(sh), 968(sh), 955(s), 836(sh), 811(vs), 785(s), 745(m), 697(s), 614(m), 586(w), 560(sh), 551(m), 526(m), 510(sh), 498(m). ^{1}H NMR (CD_3OD, 293 K): δ 7.57 (m); 7.40 (m); 3.12 (q, 6H); 1.21 (t, 9H). ^{31}P NMR (CD_2Cl_2, 300 K): δ −17.4; ^{31}P NMR (CD_2Cl_2, 223 K): δ −17.4. UV–Vis (λ_{max} (nm) (ϵ (M^{-1} cm^{-1})) in CH_3OH): 247 (2100); 367 (2500); 400 (2600); 693 (220).

TABLE 4. Bond lengths (Å) for $(CH_3)_4N[ReO(O_2C_6H_4)_2]$ (**7**)

Re(1)–O(1)	1.665(17)	Re(1)–O(2)	1.963(10)
Re(1)–O(3)	1.964(9)	Re(1)–O(2A)	1.963(10)
Re(1)–O(3A)	1.964(9)	N(1)–C(7)	1.661(38)
N(1)–C(9)	1.633(69)	N(1)–C(9A)	1.633(69)
N(1)–C(7A)	1.661(38)	O(2)–C(1)	1.360(17)
N(1)–C(11A)	1.474(53)	C(1)–C(2)	1.404(22)
O(3)–C(4)	1.356(17)	C(2)–C(3)	1.376(23)
C(1)–C(1A)	1.384(29)	C(4)–C(5)	1.375(20)
C(3)–C(3A)	1.484(32)	C(5)–C(6)	1.364(22)
C(4)–C(4A)	1.466(26)	C(7)–C(8)	1.464(40)
C(6)–C(6A)	1.554(33)		

TABLE 5. Bond lengths (Å) for $(CH_3)_4N[ReO(PPh_3)(O_2C_6H_4)_2]\cdot 2CH_3OH$ (**2**)

Re(1)–P(1)	2.468(3)	Re(1)–O(1)	1.693(8)
Re(1)–O(2)	2.041(7)	Re(1)–O(3)	2.062(9)
Re(1)–O(4)	1.977(8)	Re(1)–O(5)	2.024(7)
P(1)–C(13)	1.842(11)	P(1)–C(19)	1.824(11)
P(1)–C(25)	1.822(13)	O(2)–C(1)	1.342(15)
O(3)–C(2)	1.333(15)	O(4)–C(7)	1.352(14)
O(5)–C(8)	1 380(15)	N(1)–C(31)	1.509(15)
N(1)–C(32)	1.472(19)	N(1)–C(33)	1.502(15)
N(1)–C(34)	1.475(18)	C(1)–C(2)	1.401(18)
C(1)–C(6)	1.372(18)	C(2)–C(30)	1.410(19)
C(3)–C(4)	1.400(21)	C(4)–C(5)	1.349(22)
C(5)–C(6)	1.384(21)	C(7)–C(8)	1.378(16)
C(7)–C(12)	1.368(20)	C(8)–C(9)	1.385(16)
C(9)–C(10)	1.386(20)	C(10)–C(11)	1.356(19)
C(11)–C(12)	1.396(19)	C(13)–C(14)	1.387(17)
C(13)–C(18)	1.398(15)	C(14)–C(15)	1.391(17)
C(15)–C(16)	1.377(17)	C(16)–C(17)	1.348(20)
C(17)–C(18)	1 389(17)	C(19)–C(20)	1.362(17)
C(19)–C(24)	1.395(17)	C(20)–C(21)	1.419(19)
C(21)–C(22)	1.364(20)	C(22)–C(23)	1.345(20)
C(23)–C(24)	1.421(19)	C(25)–C(26)	1.391(17)
C(25)–C(30)	1.393(18)	C(26)–C(27)	1.379(22)
C(27)–C(28)	1.356(22)	C(28)–C(29)	1.365(21)
C(29)–C(30)	1.389(21)	C(36)–O(7)	1.369(27)
C(35)–O(6A)	1.253(17)		

$[(CH_3)_4N]^+[ReO(cat)_2(NC_5H_5)]^-$ (5)

This complex was prepared by a modification of the procedure described by Griffith for a similar complex [11]. To a suspension of **2** (2.000 g; 2.65 mmol) in 80 ml dry distilled CH_2Cl_2 was added C_5H_5N (4.193 g, 53.00 mmol) dropwise via syringe. The reaction mixture became homogeneous and after 10 min a bright green solid precipitated from the reaction mixture. After 2 h of additional stirring, a bright green product was isolated by filtration in quantitative yield and dried *in vacuo* (1.51 g, 2.65 mmol, 100%). *Anal.* Calc. for $C_{23}H_{25}N_2O_5Re\cdot 0.3CH_2Cl_2$ (mol. wt. 595.71): C, 42.84; H, 4.32; N, 4.69. Found: C, 43.01; H, 3.96; N, 4.19%. IR (KBr): 3027(w), 2962(w), 1472(vs), 1449(m), 1334(vw), 1258(s), 1235(vs), 1098(m), 1017(m), 931(s), 860(w), 794(s), 742(m), 694(w), 656(m), 626(m), 521(w). ^{1}H NMR (CD_3OD, 293 K): δ 8.54 (d, J=4.6 Hz); 7.65

(br); 7.35 (br); 6.90 (br); 6.54 (br); 3.05 (s). ^{1}H NMR (CD_2Cl_2, 203 K): δ 8.42 (m); 7.38 (m); 7.06 (m); 6.71 (m); 6.58 (m); 6.39 (m); 6.08 (t); 3.13 (s). UV–Vis (λ_{max} (nm) (ϵ (M^{-1} cm^{-1})) in CH_3OH): 225 (2300); 267 (2200); 403 (sh); 615 (140).

$[(CH_3)_4N]^+[ReO(4\text{-}Me\text{-}cat)_2(NC_5H_5)]^-$ (6)

3 (0.500 g, 0.6 mmol) and C_5H_5N (0.980 g, 12.0 mmol) were reacted in 30 ml dry distilled CH_2Cl_2 as described above for **5**. A bright green product was isolated as described above (0.223 g, 0.37 mmol, 62%). *Anal.* Calc. for $C_{23}H_{29}N_2O_5Re$ (mol. wt. 599.75): C, 46.07; H, 4.87; N, 4.67. Found: C, 46.47; H, 4.65; N, 4.29%. IR (KBr): 3448(br, w), 3028(w), 2365(w), 1483(vs), 1449(m), 1324(w), 1248(s), 1212(m), 1116(w), 930(s), 810(s), 643(m), 632(m). ^{1}H NMR (CD_3OD, 293 K): δ 8.53 (br, 2H); 7.65 (br, 2H); 7.35 (br, 1H); 6.90 (br, 4H); 6.54 (br, 4H); 3.11 (s, 12H); 2.28 (br, 6H). ^{1}H NMR (CD_2Cl_2, 203 K): δ 8.54 (m); 8.41 (br); 7.70 (m); 7.38 (br); 7.30 (m); 6.92 (d, J=7.9 Hz); 6.87 (s); 6.55 (m); 6.39 (d, J=8.2 Hz); 6.22 (m); 5.92 (d); 3.11 (s); 2.24 (s); 2.09 (s). UV–Vis (λ_{max} (nm) (ϵ (M^{-1} cm^{-1})) in CH_3OH): 220 (2500); 320 (sh); 530 (170).

$[(CH_3CH_2)_4N]^+[ReO(cat)_2]^-$ (7)

A solution of $[(CH_3CH_2)_4N]^+[ReO_2(cat)_2]^-$ (**8**) (2.000 g, 3.54 mmol) and PPh_3 (1.022 g, 3.90 mmol) was refluxed in 30 ml anhydrous ethanol. After 1 h, a tan solid precipitated from the reaction mixture. The product was collected by filtration, washed with ethanol and dried *in vacuo* (1.569 g, 2.86 mmol, 81%). *Anal.* Calc. for $C_{20}H_{28}NO_5Re$ (mol. wt. 548.70): C, 43.78; H, 5.14; N, 2.55. Found: C, 44.27; H, 4.97; N, 2.34%. IR (KBr): 3018(w), 2367(w), 1473(vs), 1229(vs), 1147(w), 1096(w), 1017(w), 973(s), 910(vw), 864(w), 800(m), 744(s), 686(w), 656(s), 550(m). ^{1}H NMR (CD_3CN, 293 K): δ 7.04 (m, 4H); 6.63 (m, 4H); 3.08 (q, J=7.3 Hz, 8H); 1.13 (t, 12H). ^{13}C NMR (CD_2Cl_2, 293 K): δ 167.1; 120.4; 113.7; 52.8; 7.1. UV–Vis (λ_{max} (nm) (ϵ (M^{-1} cm^{-1})) in CH_2Cl_2): 240 (3300); 270 (3300); 290 (3200); 475 (210).

Results and discussion

Synthesis and spectroscopic characterization

The rhenium catecholate complex $[(CH_3)_4N]^+[ReO(cat)_2]^-$ (**1**), previously reported by Dilworth *et al.* [12], was chosen as an ideal starting material to react with organohydrazines to form rhenium hydrazinocatecholate complexes. However under our conditions, $ReOCl(cat)(PPh_3)_2$ [11] precipitated from the reaction mixture as a red–brown solid. By modifying the conditions to utilize the exact stoichiometric amount of catechol and a two-fold excess of $(CH_3CH_2)_3N$, an olive-green, air-sensitive solid precipitated out of solution as described by Dilworth *et al.* [12] (eqn. (1)):

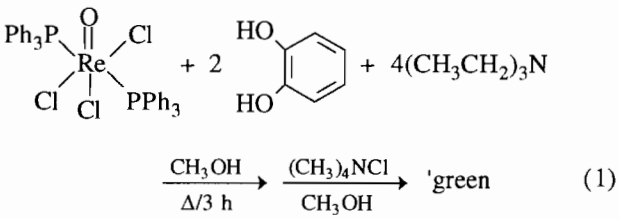

(1)

In contrast to the data reported for this complex [12], the isolated product possesses a large broad resonance at δ 7.34 in the ^{1}H NMR spectrum, whose area integrates for 15 hydrogens. This observation suggests that a PPh_3 ligand is still coordinated to rhenium and the isolated product is actually the six-coordinate complex $[(CH_3)_4N]^+[ReO(cat)_2(PPh_3)]^-$ (**2**). This was proven unequivocally by elemental analysis, ^{31}P NMR and an X-ray crystal structure (*vide infra*). Other analogs of this complex were prepared by a similar route with 4-methyl-catechol, $[(CH_3)_4N]^+[ReO(4\text{-}Me\text{-}cat)_2(PPh_3)]^-$ (**3**) and tetrachlorocatechol, $[(CH_3CH_2)_3NH]^+[ReO(Cl_4cat)_2(PPh_3)_2]^-$ (**4**). Unlike **2** and **3**, which precipitated from the reaction mixture upon addition of $(CH_3)_4NCl$, **4** precipitated directly from the reaction mixture as a triethylammonium salt.

Ligand substitution of pyridine (C_5H_5N) for PPh_3 was performed on **2** and **3** via the method of Griffith and co-workers [11] (eqn. (2)):

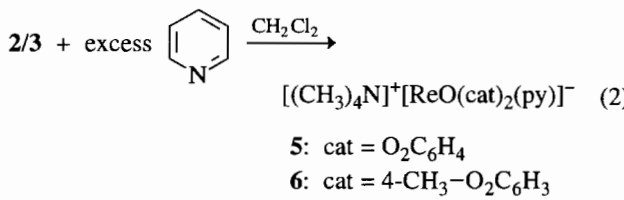

(2)

5: cat = $O_2C_6H_4$

6: cat = 4-CH_3–$O_2C_6H_3$

These complexes precipitated directly from the reaction mixture as bright green air-sensitive solids that are analytically pure.

The analytical and spectroscopic data for complexes **2–6** are tabulated in Table 6. The ^{1}H and ^{31}P NMR data for **2–6** are given in 'Experimental'. From the IR data, there are two intense stretches for the coordinated catechols attributed to the ring stretch of the C–C bond between the two donor oxygen atoms (1440–1485 cm^{-1}) and to the C–O stretch (1235–1250 cm^{-1}). For the halogeno substituted catecholate complex **4**, the C–O stretch is similar in frequency to the others reported above while the C–C stretch is considerably lower in frequency (1443 cm^{-1}) than those with unsubstituted or alkyl substituted catechols (1471–1484 cm^{-1}). This observation was also noted by Griffith and co-workers

TABLE 6. The analytical and spectroscopic data for complexes **2–7**

Complex	Analysis[a]			IR (cm^{-1})			UV–Vis (ϵ (mol^{-1} cm^{-1}))
	C	H	N	ν(CC)	ν(CO)	ν(ReO)	
2	54 07 (54.10)	4.67 (4.67)	1.86 (1.74)	1471	1237	941	220 (2300); 270 (2250); 450 (640); 647 (110)
3	53.97 (54.53)	5.05 (5.31)	1.85 (1.72)	1484	1250	937	230 (2000); 350 (sh); 530 (150)
4	40.84 (40.85)	2.80 (2.95)	1.28 (1.32)	1443	1248	955	245 (2100); 365 (2500); 400 (2600); 693 (230)
5	43 01 (42.84)	3.96 (4.32)	4.19 (4.69)	1472	1235	931	225 (2300); 270 (2300); 403 (750); 615 (150)
6	46.47 (46.07)	4.65 (4 87)	4.29 (4 67)	1483	1248	930	220 (2500), 320 (sh); 530 (170)
7	44 27 (43.78)	4.97 (5.14)	2.34 (2.55)	1473	1229	973	240 (3300); 270 (3300); 290 (3200); 475 (210)

[a]Calculated values in parentheses.

in other rhenium oxo–catecholato complexes [11]. There are no assignable ν(OH) stretches in the 3300–3600 cm^{-1} region, indicating that the catecholate ligands are deprotonated. There is also a terminal Re=O stretch in the typical region for complexes that contain a terminal rhenium–oxo bond ((930–1000 cm^{-1}) [23]. For **4**, the frequency of the ν(ReO) stretch (955 cm^{-1}) is somewhat greater than those of the other complexes above (930–941 cm^{-1}) because the electronegative Cl groups on the catecholate rings withdraws electron density away from the metal center, thereby increasing the rhenium–oxo interaction. The UV–Vis data listed in Table 6 reveal typical $\pi \rightarrow \pi^*$ transitions for the catechol rings in the UV region while either ligand to metal charge transfer bands and/or d–d transitions are observed in the visible region.

^{1}H and ^{31}P NMR spectra at variable temperatures for **2–6** exhibit behavior which is indicative of dissociation–association of the ancillary ligand PPh_3 in **2–4**; C_5H_5N in **5**, **6** with concomitant *cis–trans* isomerization of the catecholate ligands. The ^{1}H NMR spectrum for **2** at ambient temperatures has three broad resonances in the aromatic region. The resonance assigned to PPh_3 is at the exact chemical shift as that of the free ligand (δ 7.34) while the other two resonances are assigned to the catecholate ligands. The chemical shifts of the catecholate ligands correspond exactly to those of **7** ($[(CH_3CH_2)_4N]^+[ReO(cat)_2]^-$), where the catecholate ligands are *trans* to each other in a five-coordinate square pyramidal complex (*vide infra*). At 223 K, the slow exchange limit is reached and the catecholate ligands are assigned a structure corresponding to the PPh_3 ligand being *cis* to the oxo group. This is also observed in the solid state (see X-ray structure for **2**). In the ^{31}P NMR spectrum at 300 K, a broad resonance is observed at δ −5.2, which is very near the chemical shift of free PPh_3 (δ −6.0). At 223 K, the signal for coordinated PPh_3 is observed as a sharp resonance at δ −16.8, which is indicative of the PPh_3 ligand being primarily associated with the rhenium metal center at the exchange rate observed at this temperature. This chemical shift value compares favorably with the value for $ReOCl(cat)(PPh_3)_2$ (δ −17.2) observed by Griffith and co-workers [11].

For **3**, analogous behavior is observed in the ^{1}H and ^{31}P NMR spectra. However in the ^{31}P NMR spectrum at 223 K, the slow exchange limit is met and three closely spaced resonances are observed in a 1:2:1 ratio (δ −16.7; −16.8; −17.0). This observation corresponds to the four possible isomers that occur with all possible arrangements of the 4-methyl-catecholate ligands where the PPh_3 ligand is *cis* to the oxo group (**3A–3D**). Since the resonances are in a 1:2:1 ratio, the resonance at δ −16.8 (area 2) may correspond to two overlapping resonances for two of the four possible isomers. Similar behavior was observed in the low temperature ^{1}H NMR spectrum for **3** in which a multitude of resonances for the catecholate hydrogens are observed between δ 5.22–7.01 which is indicative of isomerism occurring in solution involving the different arrangements of the methyl groups on the catecholate ligands as pictured above (**3A–3D**).

For **4**, a sharp resonance is observed at δ −17.4 at 223 and 300 K in the ^{31}P NMR spectrum, which is indicative of the dissociation–association process involving the PPh_3 ligand described above being slow on the NMR timescale even at 300 K. This chemical shift value also compares favorably with the value for

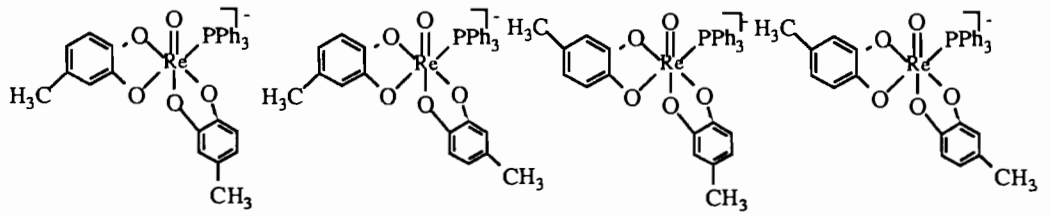

3A 3B 3C 3D

$ReOCl(Cl_4cat)(PPh_3)_2$ (δ −15.3) noted by Griffith and co-workers [11]. One reasoning for the decrease in rate for the dissociation–association process in **4** is that the electron-withdrawing ability of the Cl groups attached to the catecholate ligands renders the rhenium metal center to be more electron poor than in the other complexes studied and thereby increases the Re–P bond strength. Also, the Cl groups on the catecholate ligands might sterically hinder the twisting motion that occurs when the PPh_3 ligand dissociates and the catecholate ligands isomerize.

Analogous behavior was observed for **5** and **6** where the pyridine ligand is undergoing dissociation–association behavior in solution. At ambient temperatures, there are five broad resonances in the aromatic region for **5** and **6**. The three downfield resonances at δ 8.58, 7.64 and 7.31 correspond very closely to the chemical shifts of free pyridine while the two broad catecholate resonance are at the same chemical shift as observed in **7** (*vide infra*). At 203 K, the slow exchange limit is met where the pyridine resonances are shifted due to coordination and the number of resonances and multiplicities of the catecholate resonances are consistent with the geometry of the complex having the pyridine ligand *cis* to the oxo ligand. For **6**, two resonances for the *ortho*-hydrogens on the pyridine and two resonances for the tolyl group are observed in a 2:1 ratio indicative of two isomers or perhaps two pairs of isomers analogous to **3A–3D** above where a pyridine ligand replaces the PPh_3 ligand pictured. The trace in Fig. 1(a) illustrates the ambient temperature ^1H NMR spectrum of the aromatic region of **6** while (b) illustrates the slow exchange limiting spectrum where the number of resonances corresponding to the catecholate and pyridine ligands is indicative of isomerization analogous to **3** occurring in solution.

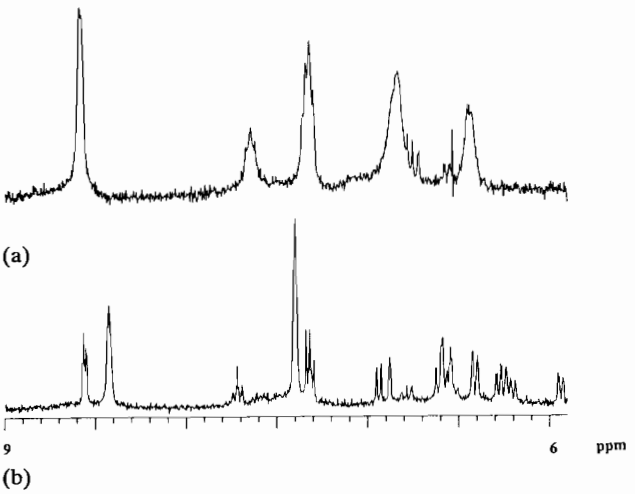

Fig. 1. The ^1H NMR spectrum for $[(CH_3)_4N]^+[ReO(4\text{-}Me\text{-}cat)_2(NC_5H_5)]^-$ (**6**) 293 (a) and 203 (b) K between 6 and 9 ppm.

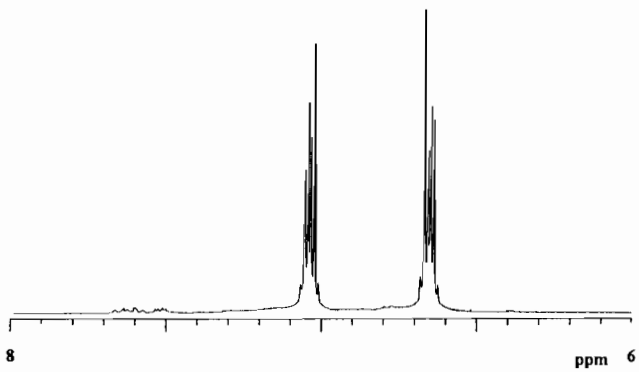

Fig. 2. The ^1H NMR spectrum for $[(CH_3CH_2)_4N]^+[ReO(cat)_2]^-$ (**7**) between 6 and 8 ppm.

All attempts to react **2–6** with either monosubstituted or 1,1-disubstituted organohydrazines under a variety of reaction conditions yielded distinct color changes but no tractable products could be isolated. One reason for this could be due to the general insolubility of the tetramethylammonium salts of the complexes. Therefore, attempts were made to prepare the $[(CH_3CH_2)_4N]^+$ and Ph_4P^+ salts of **2**, but isolation of a pure product proved to be difficult. Instead, the reduction of $[(CH_3CH_2)_4N]^+[ReO_2(cat)_2]^-$ (**8**) with excess PPh_3 to generate $[(CH_3CH_2)_4N]^+[ReO(cat)_2(PPh_3)]^-$ was attempted, but serendipitously $[(CH_3CH_2)_4N]^+[ReO(cat)_2]^-$ (**7**) was formed as a tan solid (eqn. (3)):

$$[(CH_3CH_2)_4N]^+[ReO_2(cat)_2]^- + 1.5\ PPh_3 \xrightarrow[\Delta/1\ h]{CH_3CH_2OH} [(CH_3CH_2)_4N]^+[ReO(cat)_2]^- \quad (3)$$

The complex precipitated from solution as a very air-sensitive, analytically pure tan solid.

The analytical and spectroscopic data for **7** are tabulated in Table 6. The ^1H and ^{13}C NMR data is given

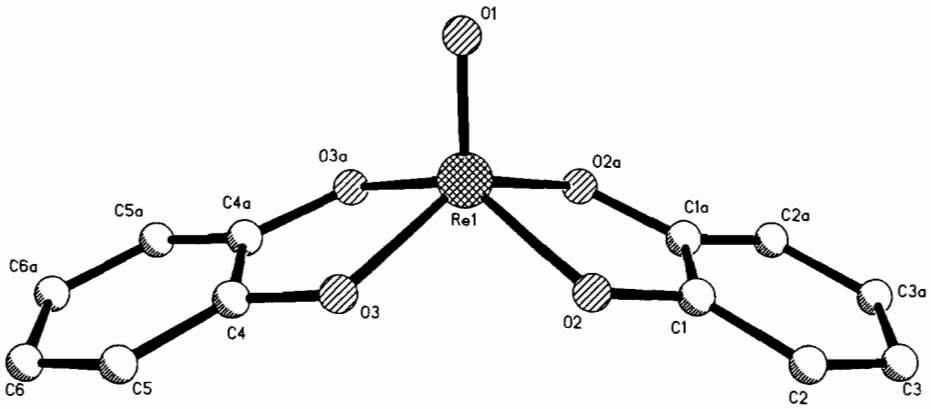

Fig. 3. A view of the structure of $[ReO(cat)_2]^-$, showing the atom labelling scheme.

TABLE 7. Comparison of bond lengths (Å) for Re(V) and Tc(V) catecholate complexes

Compound	M=O	M−O_t	M−L[a]	O=M−L	Ref.
$[ReO(O_2C_6H_4)_2]^-$	1.67(2)	1 96(1)			this work
$[TcO(O_2C_6H_4)_2]^-$	1.648(5)	1.957(4)			5
$[ReO(OPPh_3)(O_2C_6Cl_4)_2]^-$	1.576(8)	2.017(8)	2.232(6)	178.5(3)	11
$[ReO(HOMe)(O_2C_6Cl_4)_2]^-$	1.653(11)	2.000(12)	2.289(11)	179.2(4)	11
$[ReO(PPh_3)(O_2C_6H_4)_2]^-$	1.693(8)	1.977–2.062(8)	2.468(3)	87.4(3)	this work

[a]L refers to the sixth ligand in complexes of the type $[ReO(O_2C_6H_4)_2L]^-$.

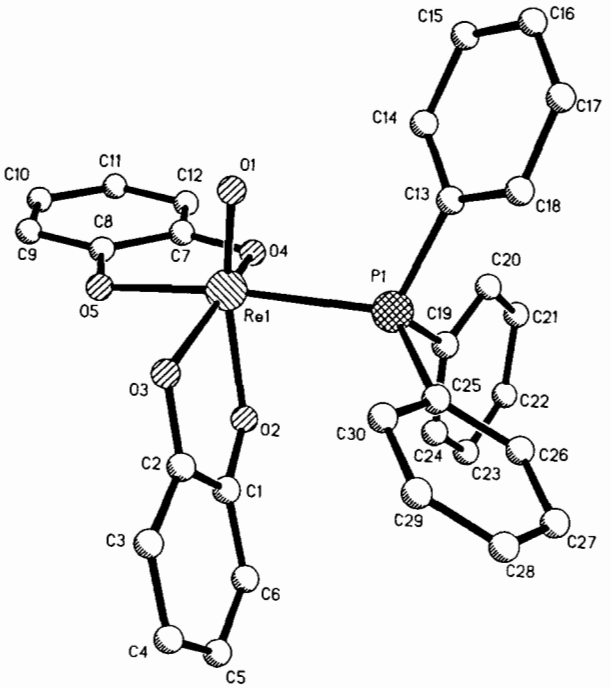

Fig. 4. A view of the structure of $[ReO(PPh_3)(cat)_2]^-$, showing the atom labelling scheme.

in 'Experimental'. IR spectroscopy reveals two intense stretches for the coordinated catecholate ligands (ν(CC): 1474 cm^{-1}; $\nu_{(CO)}$: 1230 cm^{-1}) and a ν(ReO) stretch at 973 cm^{-1}. ^1H NMR spectroscopy exhibits two multiplets at δ 7.04 for the hydrogens attached to C(3,4) of the catecholate rings and at δ 6.65 for the hydrogens attached to C(5,6) of the catecholate rings. These multiplets are coupled to each other as a second-order AA'BB' pattern (Fig. 2). While ^{13}C NMR spectra could not be measured on **2–6** due to insolubility of the $[(CH_3)_4N]^+$ salts of these complex anions, the $[(CH_3CH_2)_4N]^+$ salt of **7** was soluble enough to be measured conveniently. The ^{13}C NMR spectrum of **7** exhibits a substantial downfield coordination shift for the C(1,2) catecholate resonance at δ 167.1 as compared to the resonance for C(1,2) for non-coordinated catechol (δ 146.6). This is similar to the downfield coordination shifts that Griffith observes with C(1) and C(2) of the catecholate rings in oxo–catecholato rhenium complexes previously reported [11]. The UV–Vis spectrum exhibit two bands in the UV region for $\pi \rightarrow \pi^*$ transitions in the catechol ring while the visible bands correspond to a ligand-to-metal charge transfers.

Structures of $(C_2H_5)_4N[ReO(cat)_2]$ (7) and $(CH_3)_4N[ReO(cat)_2(PPh_3)] \cdot 2CH_3OH$ (2)

Crystals of $(C_2H_5)_4N[ReO(cat)_2]$ suitable for an X-ray crystal structure determination were grown from methylene chloride/ether as brown needles. As shown in Fig. 3, the molecular anion lies on the crystallographic mirror plane. The overall geometry is square pyramidal with the oxo group occupying the apical position and the square base defined by the four oxygen donors of

the two catecholate ligands. The structure of the anion is similar to that reported for $[TcO(cat)_2]^{4-}$, as shown by the comparison of the $\{MO_5\}$ cores for M=Tc and Re provided in Table 7. The structure of **7** may also be compared to those of the $OPPh_3$ and methanol adducts, $[ReO(OPPh_3)(Cl_4cat)_2]^-$ (**9**) and $[ReO(HOCH_3)(Cl_4cat)_2]^-$ (**10**). While the metrical parameters for $[ReO(cat)_2]^-$ and $[TcO(cat)_2]^-$ are nearly identical, the consequences of adduct formation in the $[ReO(L)(Cl_4cat)_2]^-$ derivatives ($L=OPPh_3$ and $HOCH_3$) are manifested in increased Re–O(catecholate) distances as a consequence of steric crowding about the Re centers.

The structure of the triphenylphosphine adduct **2** consists of discrete cations and molecular anions $[ReO(cat)_2(PPh_3)_2]^-$. As shown in Fig. 4, the geometry of the anion is distorted octahedral. However, in contrast to the structures of previously reported adducts, the anion of **2** exhibits phosphine coordination *cis* to the terminal oxo group, a geometry which causes rearrangement of the catecholate oxygen donors from the planar orientation of the $[ReO(cat)_2]^-$ parent to one in which one catecholate oxygen is *trans* to the terminal oxo group. It is noteworthy that there is no pronounced lengthening of the Re–O(2) bond distance as a consequence of the *trans* influence of the oxo group. This contrasts with the structural characteristics of $[ReO_2(cat)_2]^-$ where the Re–O(catecholate) distances are 2.031(7) and 1.952(6) Å for the bonds *trans* and *cis* to terminal oxo groups, respectively [12]. The *cis* orientation of the PPh_3 group relative to the Re=O unit in **2** presumably reflects the π-bonding ability of the phosphine ligand. The *cis* geometry minimizes competition between the oxo group and the phosphine for the metal t_{2g} orbitals. Since π-bonding is not expected to be significant for $HOCH_3$ or $OPPh_3$, the *trans* {O=Re–L} geometry observed for these adducts reflects the minimal structural reorganization required to accommodate the additional ligand.

Supplementary material

Details of experimental procedures are available from the authors on request.

Acknowledgement

The work at Syracuse University was supported by the US Department of Energy, Grant No. DE-FG02-93ER61571. We thank Professor James M. Mayer of the University of Washington for several useful suggestions and observations.

References

1 B.F. Matzanke, G. Müller-Matzanke and K.N. Raymond, *Siderophore Mediated Iron Transport; Chemistry, Biology and Physical Properties, Physical Biochemistry,* VCH, New York, 1989, p. 1.
2 T. Stabler, *J. Med Tech., 3* (1986) 351.
3 J. Axelrod, *J. Neurosurg., 55* (1981) 669.
4 A. Davison, B.V. DePamphlis, A.G. Jones, K.J. Franklin and C.J.L. Lock, *Inorg. Chim Acta, 128* (1987) 161.
5 M.J. Abrams, S.K. Larsen and J. Zubieta, *Inorg Chem., 30* (1991) 2031.
6 L.A. deLearie, R.C. Haltiwanger and C.G. Pierpont, *J Am. Chem. Soc, 111* (1989) 4324.
7 L.A. deLearie, R.C. Haltiwanger and C.G. Pierpont, *Inorg Chem, 26* (1987) 817.
8 W.A. Herrmann, U. Kusthardt and E. Hudtwick, *J Organomet. Chem, 294* (1985) 633.
9 J. Takacs, P. Kiprof, J. Riede and W.A. Herrmann, *Organometallics, 9* (1990) 782.
10 J. Takacs, M.R. Cooks, P. Kiprof, J.G. Kuchler and W.A. Herrmann, *Organometallics, 10* (1991) 376.
11 C.F. Edwards, W.P. Griffith, A.J.P. White and D.J. Williams, *J. Chem. Soc., Dalton Trans.,* (1992) 957.
12 J.R. Dilworth, S K. Ibrahim, S.R. Khan, M.B. Hursthouse and A.A. Karaulov, *Polyhedron, 9* (1990) 1323.
13 S.N. Brown and J.M. Mayer, *Inorg. Chem., 31* (1992) 4091.
14 M.J Abrams, S N. Shaikh and J. Zubieta, *Inorg. Chim. Acta, 173* (1990) 133.
15 M.J. Abrams, S K Larsen and J. Zubieta, *Inorg Chim. Acta, 171* (1990) 133.
16 M.J. Abrams, Q. Chen, S.N. Shaikh and J. Zubieta, *Inorg. Chim. Acta, 176* (1990) 11.
17 M.J. Abrams, S.K. Larsen, S.N. Shaikh and J. Zubieta, *Inorg. Chim. Acta, 185* (1991) 7.
18 D.A Schwartz, M.J. Abrams, M.M. Hauser, F.E. Gaul, S.K. Larsen, D. Rauh and J.A. Zubieta, *Bioconjugate Chem, 2* (1991) 333
19 M.J. Abrams, M. Juweid, C.I. ten Kate, D.A. Schwartz, M.M Hauser, F.E. Gaul, A.J. Fuccello, R.H. Rubin, H.W. Strauss and A.J. Fischman, *J. Nucl Med., 31* (1990) 2022.
20 P.B. Kettler, M.J Abrams, Y.-D. Chang and J. Zubieta, *Inorg. Chem,* submitted for publication.
21 D.D. Perrin, W.L.F. Armarego and D.R. Perrin, *Purification of Laboratory Chemicals,* Pergamon, New York, 1980.
22 G.W. Parshall, *Inorg Synth, 17* (1977) 110.
23 W.A Nugent and J.M Mayer, *Metal–Ligand Multiple Bonds,* Wiley-Interscience, New York, 1988.